Psychiatry Research: Neuroimaging xxx (2011) xxx–xxx

Contents lists available at ScienceDirect

Psychiatry Research: Neuroimaging

journal homepage: www.elsevier.com/locate/psychresns

Shape alterations in the striatum in chorea-acanthocytosis

Mark Walterfang[a,*], Jeffrey Chee Leong Looi[b], Martin Styner[c], Ruth H. Walker[c], Adrian Danek[c], Marc Neithammer[c], Andrew Evans[c], Katya Kotschet[c], Guilherme R. Rodrigues[c], Andrew Hughes[c], Dennis Velakoulis[c]

[a]Neuropsychiatry Unit, Level 2, John Cade Building, Royal Melbourne Hospital 3050, Australia
[b]Research Centre for the Neurosciences of Ageing, Academic Unit of Psychological Medicine, School of Clinical Medicine, Australian National University Medical School, Canberra Hospital, Canberra, Australia
[c]Department of Neurology, James J. Peters Veterans Affairs Medical Center, Bronx, NY 10468, USA and Department of Neurology, Mount Sinai School of Medicine, New York, NY 10029, USA

ARTICLE INFO

Article history:
Received 6 March 2010
Received in revised form 21 October 2010
Accepted 21 October 2010
Available online xxxx

Keywords:
Neuroacanthocytosis
Chorea-acanthocytosis
Chorea
Caudate
Striatum
Neurodegeneration

ABSTRACT

Chorea-acanthocytosis (ChAc) is an uncommon autosomal recessive disorder due to mutations of the *VPS13A* gene, which encodes for the membrane protein chorein. ChAc presents with progressive limb and orobuccal chorea, but there is often a marked dysexecutive syndrome. ChAc may first present with neuropsychiatric disturbance such as obsessive–compulsive disorder (OCD), suggesting a particular role for disruption to striatal structures involved in non-motor frontostriatal loops, such as the head of the caudate nucleus. Two previous studies have suggested a marked reduction in volume in the caudate nucleus and putamen, but did not examine morphometric change. We investigated morphometric change in 13 patients with genetically or biochemically confirmed ChAc and 26 age- and gender-matched controls. Subjects underwent magnetic resonance imaging and manual segmentation of the caudate nucleus and putamen, and shape analysis using a non-parametric spherical harmonic technique. Both structures showed significant and marked reductions in volume compared with controls, with reduction greatest in the caudate nucleus. Both structures showed significant shape differences, particularly in the head of the caudate nucleus. No significant correlation was shown between duration of illness and striatal volume or shape, suggesting that much structural change may have already taken place at the time of symptom onset. Our results suggest that striatal neuron loss may occur early in the disease process, and follows a dorsal–ventral gradient that may correlate with early neuropsychiatric and cognitive presentations of the disease.

1. Introduction

The *neuroacanthocytoses* are a group of disorders that present with neurological and psychiatric manifestations, and *acanthocytes*, spiculated red blood cells. *Chorea-acanthocytosis* (ChAc; MIM 200150) is an autosomal recessive disorder associated with mutations or deletions in the *VPS13A* gene on chromosome 9q. This gene codes for the membrane protein chorein (Ueno et al., 2001b; Rampoldi et al., 2002), which is strongly expressed in the brain (Dobson-Stone et al., 2002). Loss of function of chorein appears to affect basal ganglia neurons, especially those in the caudate and putamen (Bader et al., 2008). Onset of neurological disturbance in ChAc is usually between ages 25 and 45, commonly with limb chorea that may be indistinguishable from Huntington's disease (Dobson-Stone et al., 2002), but also with distinctive lingual feeding dystonia (Bader et al., 2010). Identification and sequencing of the *VPS13A* gene (Rampoldi et al., 2001; Ueno et al., 2001a) have enabled definitive diagnosis of ChAc and differentiation from related neuroacanthocytosis syndromes such as McLeod syndrome (Danek et al., 2005). Diagnosis has been facilitated by the development of a Western blot screening test for decreased or absent levels of chorein (Dobson-Stone et al., 2004).

Histopathologically, the relatively rare ChAc cases with confirmed *VPS13A* mutations have shown marked striatal neuronal loss with reactive astrocytic gliosis, particularly in the head of the caudate nucleus, with the globus pallidus less affected; and with minimal changes in the thalamus and substantia nigra, with the cortex almost universally spared (Bader et al., 2008). Magnetic resonance imaging (MRI) findings in established ChAc cases mirror these findings, showing marked striatal atrophy in the absence of significant cortical atrophy (Hardie et al., 1991; Kutcher et al., 1999; Walterfang et al., 2008).

The functional consequences of these changes in the striatum are the characteristic choreiform movements, thought to be the result of disruption of motor loops in the putamen and pallidum (Danek et al., 2005), and behavioural and neuropsychiatric symptoms. The involvement of non-motor frontostriatal loops that run through the caudate nucleus, in particular, may be responsible for the characteristic executive impairment seen in the illness (Hardie et al., 1991; Danek et al., 2005). Patients with ChAc have very high rates of obsessive–

* Corresponding author. Tel.: +61 393428750; fax: +61 393428483.
E-mail address: mark.walterfang@mh.org.au (M. Walterfang).

0925-4927/$ – see front matter © 2010 Elsevier Ireland Ltd. All rights reserved.
doi:10.1016/j.pscychresns.2010.10.006

compulsive disorder (Walterfang et al., 2008), unique for any neurodegenerative condition, suggesting disruption to the caudate's central role in the function of the lateral orbitofrontal loop (LOFL) in subserving the choice of behavioural actions relevant to emotional and cognitive inputs from frontal cortex (Chamberlain et al., 2005).

Aside from case reports, only two systematic analyses of striatal volume have been undertaken in ChAc patients. Henkel et al. used a voxel-based morphometry (VBM) approach to compare six ChAc patients to 15 age-matched controls, and showed a focal and symmetrical atrophy of the caudate nucleus, but no reduction in any other brain region, including in the putamen (Henkel et al., 2006). Huppertz et al. expanded the dataset to nine ChAc patients, and utilised the normalization component of the VBM approach of Henkel et al. to create caudate and putamen masks from a large control group average to determine normalized volume of these structures. They demonstrated a significant volumetric reduction in both structures, and showed complete separation of ChAc patients and controls on measures of caudate volume (Huppertz et al., 2008). However, the methodology of these studies did not extend beyond analysing the total volume of striatal structures in ChAc. One study analysed striatal volume in three brothers with McLeod syndrome (a related neuroacanthocytosis syndrome) and 20 matched controls, and showed that patients' striatal volumes were significantly reduced compared with those of controls, with caudate nuclei showing a trend towards significant volume reduction over a 7-year follow-up period (Valko et al., 2010).

We sought to confirm and extend upon the findings of Huppertz et al. (2008) with an expanded dataset, using a standardized and validated traditional manual tracing methodology for each structure, followed by a morphometric analysis to determine whether the shape or morphology of the caudate and putamen differed between ChAc patients and controls. This allowed us to explore whether there are regional neuroanatomical changes to striatal structures in ChAc that may relate to the characteristic symptoms of the illness. Our hypothesis was that the caudate nucleus would be disproportionately affected, and that we would find a predilection for involvement of the head of the caudate nucleus, in particular regions that form a crucial component of the LOFL, in the patient group.

2. Materials and methods

2.1. Subjects

Patients with ChAc ($n=13$) were recruited from multiple centres worldwide, including the United Kingdom, Europe, North and South America, and Australia. Patients 1–8 include the six patients described in the previously published VBM study (Henkel et al., 2006) and patients 1–7 reported by Huppertz et al. (2008). Patient 9 has been previously described by Robertson et al. (2008a) and Walterfang et al. (2008a), and patient 11 corresponds to case 2 of Rodrigues et al. (2008b). Patients 12 and 13 are two previously unpublished siblings from Australia. Molecular genetic diagnosis was confirmed by mutations in the *VPS13A* gene, abnormally reduced chorein expression by Western blot, or both. In addition, 4/13 patients had obsessive–compulsive symptoms or disorder, and 11/13 had executive dysfunction. Controls ($n=26$) were matched two-for-one for age and gender to the patient sample, and were selected from a large database of healthy normal controls recruited by hospital and media advertisements by the Melbourne Neuropsychiatry Centre.

2.2. MRI scanning

High-resolution volume-rendering 3D datasets of the whole head were obtained for all subjects for the purpose of manual volumetry. All control subjects were scanned on a 1.5T General Electric Signa MRI scanner (GE, Milwaukee, USA) at the Royal Melbourne Hospital, Melbourne. Images were acquired in the axial plane using a T_1 weighted, 3D Spoiled Gradient Recalled Echo (SPGR) protocol (slice thickness = 1.5mm, in plane resolution = 0.9375 mm×0.9375 mm). ChAc subjects 1–9 were also scanned on a 1.5T General Electric Signa scanner, using a similar SPGR sequence; patient 10 was scanned on a 1.5T Siemens Magnetom Vision Plus and patients 11–13 on a 1.5T Siemens Avanto, using a T_1 weighted, 3D Magnetized Prepared RApid Gradient Echo (MPRAGE) protocol (slice thickness = 1 mm, in plane resolution = 1 mm × 1 mm). As ChAc patients were scanned on different machines, the signal-to-noise ratio (SNR) was calculated for each scan using regions-of-interest in left prefrontal white matter (WM) and in the image background (BG). SNR was calculated as the mean of the WM signal divided by the standard deviation of the BG signal. The SNR between controls (0.0447 ± 0.0123) and ChAc patients (0.0509 ± 0.0246) was not significantly different ($p=0.307$).

2.3. Image processing

Images were transferred to an Intel Apple MacBook Pro computer running OSX 10.5 (Apple Inc, Cupertino, CA, USA), and were checked manually for gross structural abnormalities prior to analysis. The software ANALYZE 9.0 (Mayo BIR, Rochester, MN, USA) was used for image analysis. Images were rescaled to isotropic format ($1 \times 1 \times 1$ mm^3). Manual segmentation was axially performed using a standardized view, rigidly aligned in the AC-PC plane. All brain scans were analysed blindly to all clinical information by an experienced rater (JCLL, Fig. 1). A standardized manual tracing protocol was used to trace and quantify the volume of the caudate via tracing its axial outline serially through successive images (Looi et al., 2008). Intra-rater class correlation was established at 0.97 for this rater (Looi et al., 2008). We then adapted a reference image-based protocol developed previously for a study of the putamen in frontotemporal lobar degeneration (Looi et al., 2009). Intra-rater class correlation was 0.93 for this rater (Looi et al., 2009). Inter-rater reliability with another experienced tracer using this method was rated at 0.98 for the caudate and 0.87 for the putamen (Looi et al., 2008; Looi et al., 2009). Volumes obtained were normalized in relevant analyses by calculation of total intracranial volume (ICV). We then calculated *Z*-scores for all subjects based on the mean and standard deviation volume measures from the control group, as in a previous analysis of ChAc patients (Huppertz et al., 2008). Total ICV was measured by a stereological point counting technique manually tracing the intracranial volume, with every fourth slice traced. The starting point was randomly chosen from the most anterior four brain slices. The landmarks for delineation and protocol are based upon those previously published (Eritaia et al., 2000).

2.4. Shape analysis

Shape analysis was undertaken in a semi-automated fashion using the University of North Carolina shape analysis toolkit (Styner et al., 2006; Paniagua et al., 2009), a technique that has been used in a range of studies in neuropsychiatric illness (Styner et al., 2004; Zhao et al., 2008; Levitt et al., 2009). Segmented 3D label maps are initially processed to ensure that interior holes are filled, followed by morphological closing and minimal smoothing. These are then subjected to spherical harmonic shape description (SPHARM-PDM), with reconstructed boundary surfaces of all segmentations mapped onto the unit sphere and described via a set of coefficients weighting spherical harmonic basis functions. The correspondence between surfaces is established by a parameter-based rotation based on first-order expansion of the spherical harmonics. All surfaces are then uniformly sampled into sets of 1002 surface points each. These surfaces are aligned to a study-averaged template for each structure (left and right caudate and putamen) using rigid-body Procrustes alignment (Bookstein, 1997), with normalization for head size

Please cite this article as: Walterfang, M., et al., Shape alterations in the striatum in chorea-acanthocytosis, Psychiatry Research: Neuroimaging (2011), doi:10.1016/j.pscychresns.2010.10.006

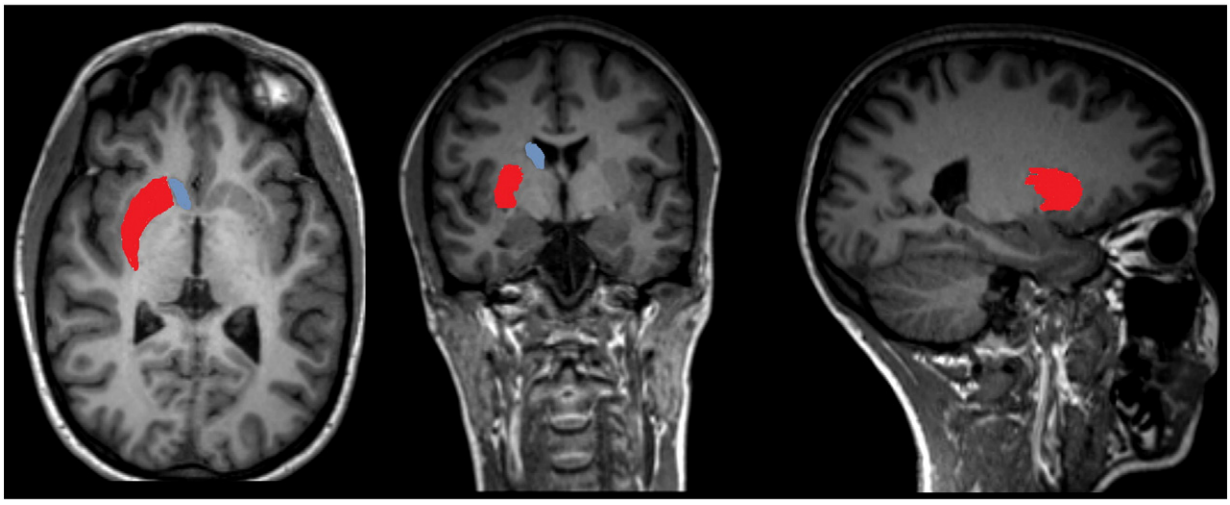

Fig. 1. Representation of orientation of caudate (red) and putamen (blue) shapes on coronal, sagittal and horizontal view of a healthy control brain. It is not possible to visualize both the caudate and putamen in the sagittal view; thus, in this view only the putamen is shown.

corrected for using ICV via a scaling factor, f_i, where $f_i = (\text{Mean (ICV)}/\text{ICV}_i)^{1/3}$.

2.5. Statistical analysis

Analysis for between-group differences in continuous demographic variables was undertaken with independent *t*-tests. Individual striatal volumes were compared using analysis of covariance (ANCOVA), covarying for ICV. To analyze a differential effect of side (left and right) and structure (caudate and putamen) between groups, we undertook a repeated-measures analysis of covariance (RM-ANCOVA) using side and structure as within-subject factors, covarying for ICV. To examine the effect of duration of illness, we examined Spearman's correlation coefficient. To compare structural shape between ChAc patients and controls, we computed the local Hotelling T_2 two-sample mean difference, and corrected for multiple comparisons using false discovery rate (FDR) (Genovese et al., 2002). We generated mean difference magnitude displacement maps and significance maps of the local *p*-values in raw format, and corrected for multiple comparisons. We also computed an overall, global shape difference summarizing the group differences across surface maps via averaging. Correlation with illness variables was performed locally based on Spearman's rank-order correlation of the projection of the surface points onto the group average surface normal. Raw and corrected *p*-values were calculated as per group differences, and displacement and significance maps were generated.

3. Results

3.1. Demographic and symptom data

The characteristics of the patient group are presented in Table 1, and between-group comparisons of demographic and volumetric data in Table 2. The patient group was not significantly different in age ($t = -0.418$, $p = 0.680$) and was identical in gender mix. The mean duration of illness in the patient group was 12.57 ± 6.87 years.

3.2. Volumetric data

Whilst ICV was 9% smaller in the ChAc group, this was not significant ($t = -1.692$, $p = 0.107$). However, individual striatal structures were all significantly smaller in the ChAc group, by 55–60% (Figs. 2 and 3, Table 2). All structures were significant at $p < 0.0001$. A *Z*-score of −2 separated all ChAc patients from controls at the caudate level, and all but patients 12 and 13, two sisters, in the putamen. RM-ANCOVA showed a main effect of group ($p < 0.0001$) and a structure-by-group interaction ($F = 7.735$, $p < 0.01$), but no side-by-group ($F = 0.038$, $p = 0.845$), structure-by-side ($F = 0.161$, $p = 0.691$) or structure-by-side-by-group interaction ($F = 0.043$, $p = 0.846$). There were no significant correlations between duration of illness and left ($r = -0.190$, $p = 0.950$) or right ($r = -0.036$, $p = 0.950$) caudate volume, nor for left ($r = -0.157$, $p = 0.608$) or right ($r = -0.246$, $p = 0.419$) putamen volume. There was no effect of scanner type (GE vs. Siemens) on volume.

3.3. Shape analysis

Shape analysis demonstrated significant changes in both structures. An overall shape difference between groups was shown for the left caudate ($p < 0.0001$), right caudate ($p < 0.0001$), left putamen ($p < 0.0001$) and right putamen ($p < 0.0001$). In the caudate, regional shape differences were seen in both left and right caudates (Fig. 4), with the most significant findings occurring in the caudate head. In the left putamen, significant changes were seen in the dorsolateral and ventral regions, and in the right putamen in the area of the dorsomedial and lateral regions (Fig. 5). There was no significant correlation between duration of illness and changes in the caudate (Fig. 6) or the putamen (Fig. 7).

Table 1
Demographic and symptom data of ChAc group. Patients 1–7 correspond with patients 1–7 from Huppertz et al. (2008). Patient 9 was described in Robertson et al. (2008b) and patient 11 in Rodrigues et al. (2008a).

	Age at scan (years)	Gender	Disease duration (years)	Diagnostic method[a]
P1	30	F	6	VPS13A
P2	42	M	18	VPS13A
P3	35	M	8	VPS13A
P4	26	M	6	VPS13A
P5	36	M	7	VPS13A
P6	40	F	18	VPS13A
P7	44	M	7	VPS13A
P8	36	M	5	Chorein
P9	38	F	17	Chorein
P10	40	M	11	Chorein
P11	59	F	30	Chorein
P12	42	F	9	Chorein
P13	46	F	12	Chorein
	39.07 ± 7.92	(7M/6F)	12.57 ± 6.87	

[a] "VPS13A" indicates that mutation was found on genetic screening. "Chorein" indicates that diagnosis was made by Western blot.

Please cite this article as: Walterfang, M., et al., Shape alterations in the striatum in chorea-acanthocytosis, Psychiatry Research: Neuroimaging (2011), doi:10.1016/j.pscychresns.2010.10.006

Table 2
Between-group comparisons on demographic and intracranial variables. t = value of t-statistic. F = value of F statistic where df = degrees of freedom.

	Patients	Controls	t/F (df)	p
Age (years)	38.02 ± 6.94	39.07 ± 7.92	−0.418 (37)	0.680
Gender (M/F)	7/6	14/12	–	–
Intracranial volume ($\times 10^3$ mm^3)	1478 ± 146	1594 ± 233	−1.692 (37)	0.107
Left caudate volume (mm^3)	1527 ± 499	4344 ± 573	154.51 (38)	<0.0001
Right caudate volume (mm^3)	1547 ± 549	4360 ± 542	152.09 (38)	<0.0001
Left putamen volume (mm^3)	1631 ± 649	3913 ± 616	78.36 (38)	<0.0001
Right putamen volume (mm^3)	1703 ± 730	3945 ± 672	58.13 (38)	<0.0001

4. Discussion

We have corroborated and extended the findings of two previous studies examining striatal volume in ChAc (Henkel et al., 2006; Huppertz et al., 2008), demonstrating in the largest cohort to date that both caudate and putaminal volumes are markedly reduced bilaterally in ChAc. This reduction in volume was greater for the caudate nuclei than for the putamen. Additionally, we showed that there was a significant morphometric difference for both structures between controls and ChAc cases, suggesting that each structure is not uniformly reduced. Significance maps showed that this was most notable for the head of the caudate nucleus, and for the dorsal aspect of the putamen.

The original VBM study suggested that volumetric reductions were confined to the head of the caudate nucleus in a small cohort of six ChAc patients compared with 15 controls (Henkel et al., 2006). We showed that caudate changes occurred in other regions beyond the head, including the tail. Our findings showing marked putaminal changes contrast to those of one other study using regional volumetry, which showed significant, but less marked, volumetric reductions in the putamen in ChAc (Huppertz et al., 2008). The lack of detection of reduction beyond the caudate head and in the putamen in a VBM-style approach may indicate an under-powered sample size (Whitwell, 2009).

The study by Huppertz et al. used similar VBM-style principles to the Henkel et al. study, and compared a larger cohort of nine ChAc patients with 257 controls. In this study all subjects' brains were normalized to a standard template, and then multiplied by a binary mask created by manual tracing of caudate and putamen on each side of a normalized average of a further 120 controls, to result in volume measures. Whilst this approach addressed the power issue inherent in the original study by use of a very large, presumably unmatched, healthy control sample, this method again presumes accurate registration of subcortical structures and that the whole putamen and caudate in each subject are contained within the grey matter mask. Nonetheless, the results of the current study are similar in the degree of volumetric reduction observed in the Huppertz et al. (2008) cohort, and we showed a similar separation of patients from controls. This may be, in part, due to the overlap between our sample and the sample analysed in these two studies. The lack of a correlation between duration of illness in our cohort is notable, however, and may be indicative of the relatively reduced spread of volumes in ChAc, or reflect the difficulty in ascertaining onset of illness when this may be related to psychiatric as well as neurologic symptom onset (Walterfang et al., 2008). Alternatively, it is possible that much of the neuron loss has already occurred at the time of illness onset (Huppertz et al., 2008). This can be contrasted to the findings in the McLeod disease study, which showed striatal volume loss occurring with illness progression (Valko et al., 2010).

Shape analysis of the caudate nucleus suggested a dorsal to ventral gradient of atrophy, combined with a caudal to rostral pattern of atrophy in patients with ChAc. These changes appear more pronounced on the left, although direct side-to-side comparisons of shape were not undertaken. A dorsal–ventral pattern of atrophy has been previously described in Huntington's disease (Douaud et al., 2006), and suggests that ChAc shares a pattern of atrophy with other neurodegenerative diseases affecting the caudate nucleus. The marked loss of neurons in the tail of the caudate nucleus may be a reflection of the relative thinness of this section in the normal state, such that a moderate loss of neurons in this region would result in a

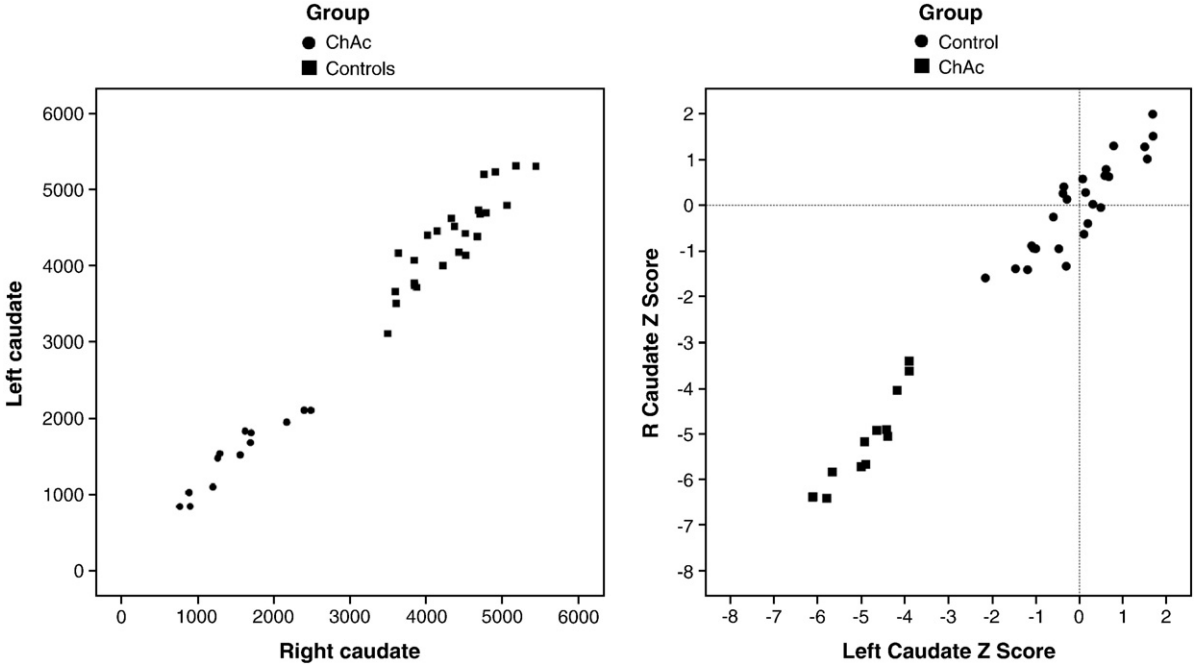

Fig. 2. Scatter plot of left and right caudate volumes (left) and Z-scores (right) according to group, showing significant separation of diagnostic groups and tight relationship between contralateral volumes.

Please cite this article as: Walterfang, M., et al., Shape alterations in the striatum in chorea-acanthocytosis, Psychiatry Research: Neuroimaging (2011), doi:10.1016/j.pscychresns.2010.10.006

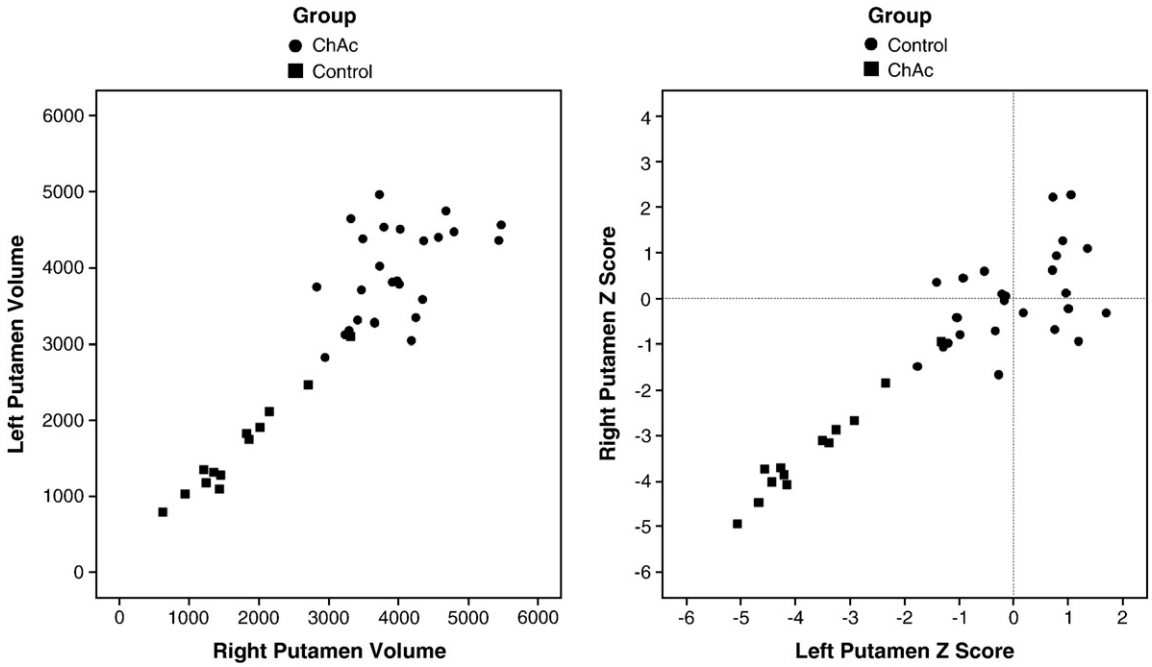

Fig. 3. Scatter plot of left and right putaminal volumes (left) and *Z*-scores (right) according to group, showing significant separation, but greater left–right variation in the control group.

marked apparent reduction and "foreshortening" of the caudate. The significantly affected regions of the rostral aspect of the left caudate nucleus receive inputs from the dorsolateral prefrontal cortex (DLPFC), anterior cingulate/medial prefrontal (ACC) and rostral motor cortex. The affected regions of the caudal left caudate nucleus receive inputs from the premotor, DLPFC and orbitofrontal (OFC) cortex (Haber et al., 2000; Haber, 2003; Leh et al., 2007; Draganski et al., 2008; Utter and Basso, 2008). For the rostral aspect of the right caudate nucleus, similar regions are involved as for the left, but to a lesser extent, whilst little caudal involvement is evident.

The putamen demonstrated a caudal to rostral pattern of atrophy in patients with ChAc, with atrophy greatest at the caudal end of the putamen on both sides. There is little evidence of a dorsal to ventral pattern of atrophy, as found in the caudate. As for the caudate nucleus, the left putamen shows a greater differential change than the right. As there was an interaction between group and side for these structures

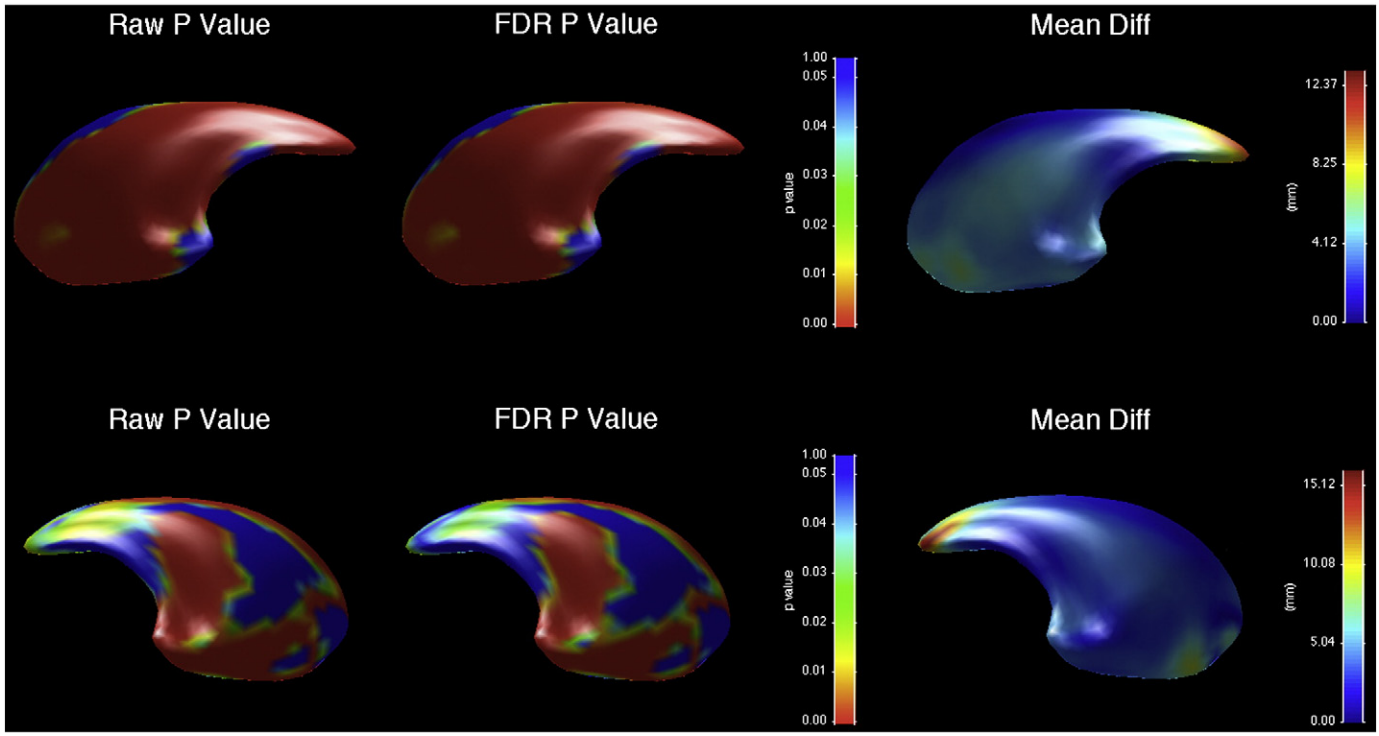

Fig. 4. Left (top) and right (bottom) caudate changes, showing differences between ChAc patients and controls. On left, uncorrected raw *p*-value map; middle, FDR-corrected *p*-value map; right, between-group displacement map. Legend to *p*-value map shows that regions with $p > 0.05$ are coloured blue, with significant values on a spectrum from green ($p = 0.05$) to red ($p = 0$). Legend to displacement map shows displacement of the ChAc group from the control group in mm.

Please cite this article as: Walterfang, M., et al., Shape alterations in the striatum in chorea-acanthocytosis, Psychiatry Research: Neuroimaging (2011), doi:10.1016/j.pscychresns.2010.10.006

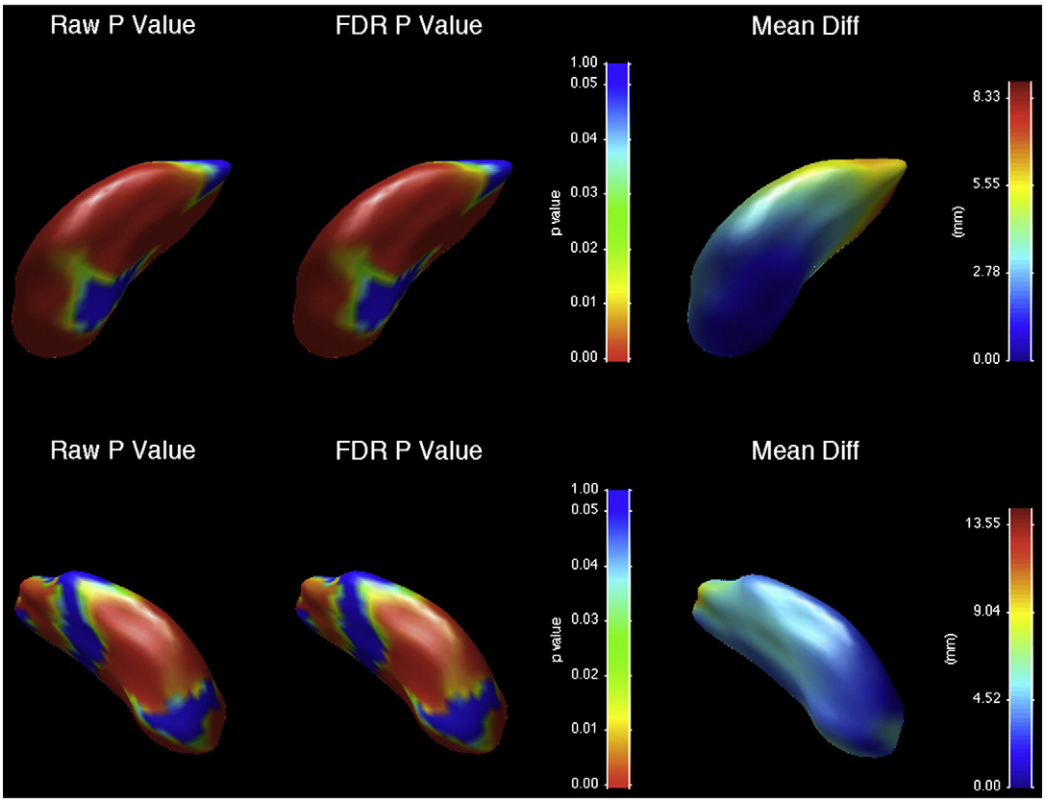

Fig. 5. Left (top) and right (bottom) putamen changes, showing differences between ChAc patients and controls. On left, uncorrected raw *p*-value map; middle, FDR-corrected *p*-value map; right, between-group displacement map. Legend to *p*-value map shows that regions with $p>0.05$ are coloured blue, with significant values on a spectrum from green ($p=0.05$) to red ($p=0$). Legend to displacement map shows displacement of the ChAc group from the control group in mm.

on measures of absolute volume, this suggests that shape rather than volume changes may be greater on the left side. Similar to the caudate nucleus, the putamen showed atrophy in regions receiving projections from DLPFC, ACC and OFC (Haber, 2003). The relative caudal atrophy of the putamen occurs in regions receiving inputs from the premotor and motor cortex and the somatosensory and supplementary motor cortex.

The atrophy described indicates potential widespread disruption of all three major frontostriatal circuits (involving the DLPFC, ACC, and OFC regions (Haber et al., 2000; Haber, 2003; Leh et al., 2007; Draganski et al., 2008; Utter and Basso, 2008)) relevant to behaviour and cognition (Tekin and Cummings, 2002; Bonelli and Cummings, 2007). These findings provide a structural basis for the clinical features

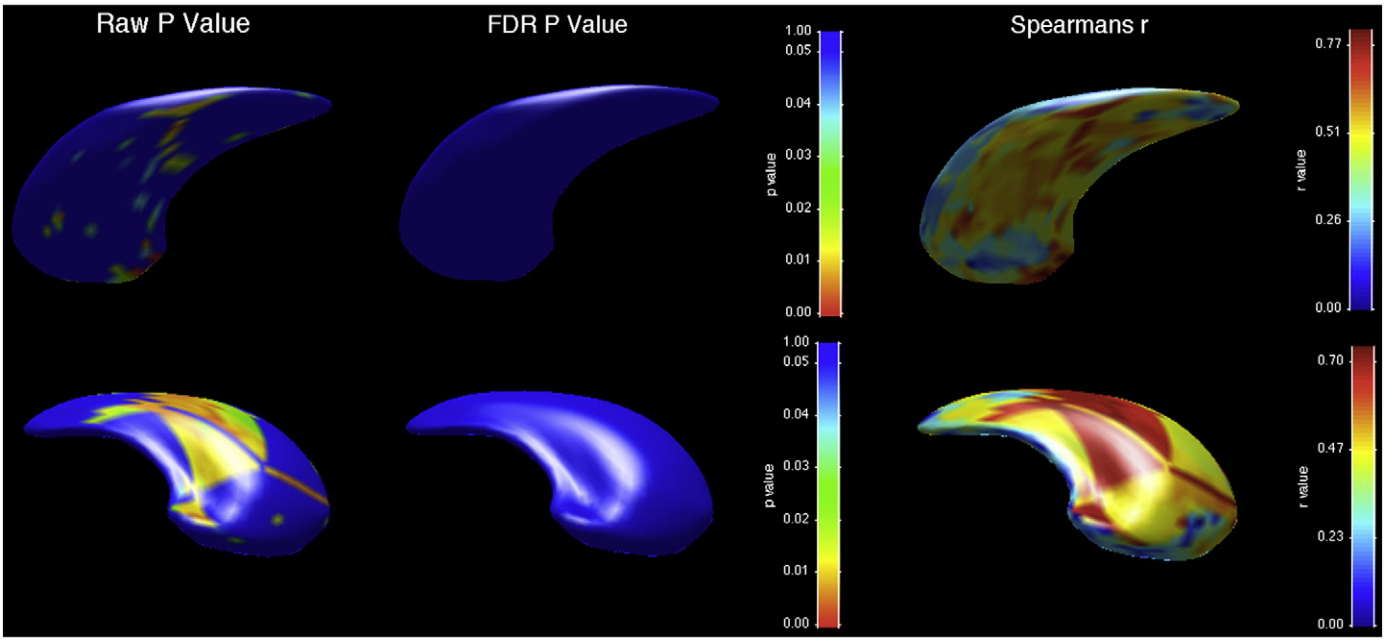

Fig. 6. Significance maps of correlations between duration of illness and shape of left (top) and right (bottom) caudates, showing uncorrected *p*-value maps (left), with FDR-corrected maps (middle) and Spearman's *r* map (right). Legend to *p*-value map shows that regions with $p>0.05$ are coloured blue, with significant values on a spectrum from green ($p=0.05$) to red ($p=0$).

Please cite this article as: Walterfang, M., et al., Shape alterations in the striatum in chorea-acanthocytosis, Psychiatry Research: Neuroimaging (2011), doi:10.1016/j.pscychresns.2010.10.006

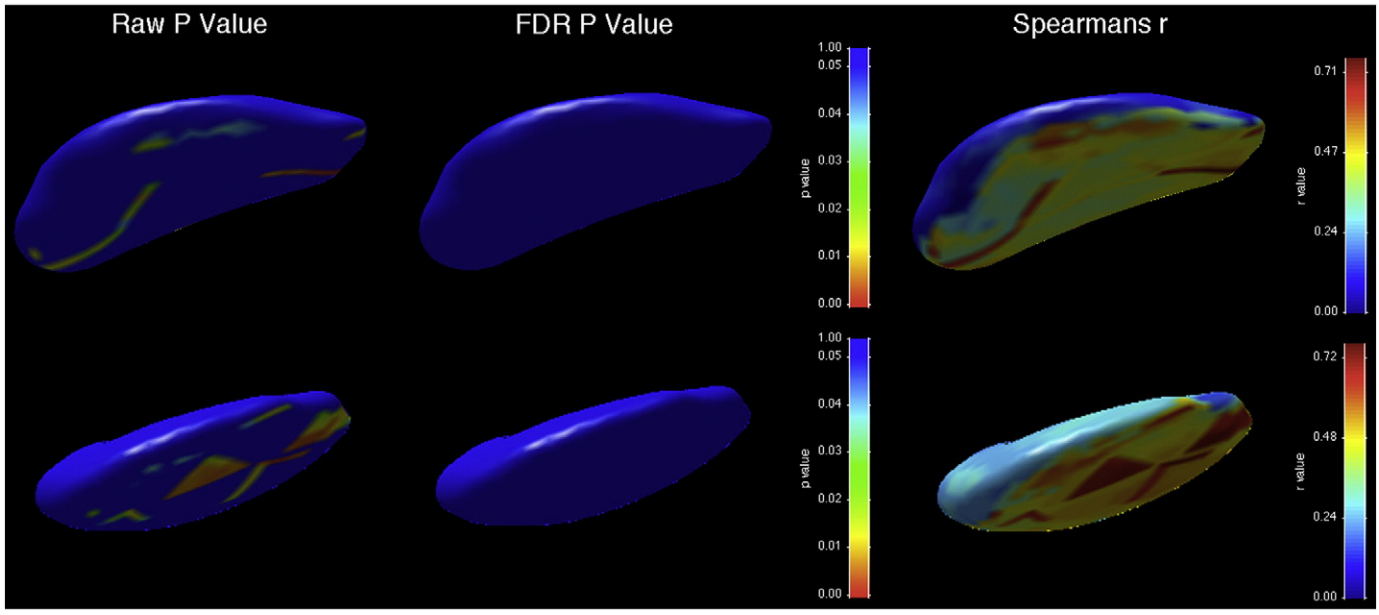

Fig. 7. Significance maps of correlations between duration of illness and shape of left (top) and right (bottom) putamen, showing uncorrected *p*-value maps (left), with FDR-corrected maps (middle) and Spearman's *r* map (right). Legend to *p*-value map shows that regions with $p>0.05$ are coloured blue, with significant values on a spectrum from green ($p=0.05$) to red ($p=0$).

of ChAc, where the most common neuropsychiatric presentation is of behavioural change consistent with a dysexecutive syndrome seen in more than 50% of cases, and the frequent presentation of OCD (Hardie et al., 1991; Walterfang et al., 2008).

4.1. Limitations

Because of the exceptional rarity of the disorder, it was necessary to acquire scans from different centres to facilitate analysis. Whilst all were scanned at 1.5T field strength and the majority of scans utilised SPGR sequences, scanner make differed amongst subjects, although it had no effect on regional striatal volume.

Whilst the nature of our shape analysis is suggestive of a particular pattern of atrophy, particularly affecting the caudate head and with greater shape changes suggested on the left, it is possible that the shape changes we see are a reflection of a process that occurs relatively uniformly across the structure. Given that the caudate is a C-shaped structure with a bulbous head and long sweeping tail, a marked uniform loss of volume due to cell death and gliosis may result in a structure with a more uniform thickness than that seen in healthy controls. Only longitudinal studies, ideally from an early or presymptomatic stage, would be able to resolve these two possibilities, to confirm whether at different illness stages differing neuronal populations are more vulnerable to disruption of normal chorein function.

4.2. Conclusion

We have corroborated previous findings suggesting a marked loss of volume in the caudate nucleus and putamen that allows almost complete separation from healthy matched controls on volumetric measures. Clear shape differences were present in ChAc patients compared with controls, suggestive of a predilection for neuronal loss of the head of the caudate nucleus. This may correlate with the findings of very high rates of dysexecutive syndromes and obsessive–compulsive symptomatology in this disorder. A lack of relationship with duration of illness in a cohort of symptomatic patients suggests that a significant volumetric loss may occur presymptomatically. We suggest that prospective, longitudinal studies be conducted to investigate morphometric change of the striatum over the course of the illness. Contemporaneous collection of neuropsychological and clinical data will allow examination of correlations of such morphometry with clinical features, enhancing our understanding of the pathophysiology of ChAc.

Financial disclosures

The authors declare they have no financial conflict of interest.

Acknowledgements

Dr Walterfang was supported by a grant from the Advocacy for Neuroacanthocytosis Patients (www.naadvocacy.org). Dr Walterfang takes responsibility for the integrity of the data and the accuracy of the data analysis. Furthermore, Dr Styner's work was funded by the UNC Neurodevelopmental Disorders Research Centre HD 03110, and the NIH Roadmap Grant U54 EB005149-01, National Alliance for Medical Image Computing. Dr. B. Bader performed the chorein Western blot with the help of G. Kwiatkowski at the Zentrum für Neuropathologie und Prionforschung, University of Munich (director: Prof. Dr. H. Kretzschmar), financially supported by the Advocacy for Neuroacanthocytosis Patients. Dr. Looi self-funded travel and accommodation for his contribution to this project at Melbourne Neuropsychiatry Centre.

References

Bader, B., Arzberger, T., Heinsen, H., Dobson-Stone, C., Kretzschmar, H., Danek, A., 2008. Neuropathology of chorea-acanthocytosis. In: Walker, R., Saiki, S., Danek, A. (Eds.), Neuroacanthocytosis Syndromes II. Springer, Heidelberg.

Bader, B., Walker, R.H., Vogel, M., Prosiegel, M., McIntosh, J., Danek, A., 2010. Tongue protrusion and feeding dystonia: a hallmark of chorea-acanthocytosis. Movement Disorders 25 (1), 127–129.

Bonelli, R., Cummings, J., 2007. Frontal-subcortical circuitry and behavior. Dialogues in Clinical Neuroscience 9, 141–151.

Bookstein, F., 1997. Shape and the information in medical images: a decade of the morphometric synthesis. Computer Vision and Image Understanding 66, 97–118.

Chamberlain, S., Blackwell, A., Fineberg, N., Robbins, T., Sahakian, B., 2005. The neuropsychology of obsessive–compulsive disorder: the importance of failures in cognitive and behavioural inhibition as candidate endophenotypic markers. Neuroscience and Biobehavioral Reviews 29, 399–419.

Danek, A., Jung, H., Melone, M., Rampoldi, L., Broccoli, V., Walker, R., 2005. Neuroacanthocytosis: new developments in a neglected group of dementing disorders. Journal of the Neurological Sciences 229–230, 171–186.

Please cite this article as: Walterfang, M., et al., Shape alterations in the striatum in chorea-acanthocytosis, Psychiatry Research: Neuroimaging (2011), doi:10.1016/j.pscychresns.2010.10.006

Dobson-Stone, C., Danek, A., Rampoldi, L., Hardie, R., Chalmers, R., Wood, N., Bohlega, S., Dotti, M., Federico, A., Shizuka, M., Tanaka, M., Watanabe, M., Ikeda, Y., Brin, M., Goldfarb, L.G., Karp, B.I., Mohiddin, S., Fananapazir, L., Storch, A., Fryer, A.E., Maddison, P., Sibon, I., Trevisol-Bittencourt, P.C., Singer, C., Caballero, I.R., Aasly, J.O., Schmierer, K., Dengler, R., Hiersemenzel, L.P., Zeviani, M., Meiner, V., Lossos, A., Johnson, S., Mercado, F.C., Sorrentino, G., Dupré, N., Rouleau, G.A., Volkmann, J., Arpa, J., Lees, A., Geraud, G., Chouinard, S., Németh, A., Monaco, A.P., 2002. Mutational spectrum of the CHAC gene in patients with choreoacanthocytosis. European Journal of Human Genetics 10, 773–781.

Dobson-Stone, C., Velayos-Baeza, A., Filippone, L., Westbury, S., Storch, A., Erdmann, T., Wroe, S., Leenders, K., Lang, A., Dotti, M., Federico, A., Mohiddin, S., Fananapazir, L., Daniels, G., Danek, A., Monaco, A., 2004. Chorein detection for the diagnosis of chorea-acanthocytosis. Annals of Neurology 56, 299–302.

Douaud, G., Gaura, V., Ribiero, M.-J., Lethimonnier, F., Maroy, R., Verny, C., Krystkowiak, P., Damier, P., Bachoud-Levi, A.-C., Hantraye, P., Remy, P., 2006. Distribution of grey matter atrophy in Huntington's disease: a combined ROI and voxel-based morphometric study. Neuroimage 32, 1562–1575.

Draganski, B., Kherif, F., Kloppel, S., Cook, P., Alexander, D., Parker, G., Deichmann, R., Ashburner, J., Frackowiak, R., 2008. Evidence for segregated and integrative connectivity patterns in the human basal ganglia. The Journal of Neuroscience 28, 7143–7152.

Eritaia, J., Wood, S., Stuart, G., Bridle, N., Dudgeon, P., Maruff, P., Velakoulis, D., Pantelis, C., 2000. An optimized method for estimating intracranial volume from magnetic resonance images. Magnetic Resonance in Medicine 44, 973–977.

Genovese, C., Lazar, N., Nichols, T., 2002. Thresholding of statistical maps in functional neuroimaging using the false discovery rate. Neuroimage 15, 870–878.

Haber, S., 2003. The primate basal ganglia: parallel and integrative networks. Journal of Chemical Neuroanatomy 26, 317–330.

Haber, S., Fudge, J., McFarland, N., 2000. Striatonigrostriatal pathways in primates form an ascending spiral from the shell to the dorsolateral striatum. The Journal of Neuroscience 20, 2369–2382.

Hardie, R.J., Pullon, H.W., Harding, A.E., Owen, J.S., Pires, M., Daniels, G.L., Imai, Y., Misra, V.P., King, R.H., Jacobs, J.M., Tippet, P., Duchen, L.W., THomas, P.K., Marsden, C.D., 1991. Neuroacanthocytosis. A clinical, haematological and pathological study of 19 cases. Brain 114 (Pt 1A), 13–49.

Henkel, K., Danek, A., Grafman, J., Butman, J., Kassubek, J., 2006. Head of the caudate nucleus is most vulnerable in chorea-acanthocytosis: a voxel-based morphometry study. Movement Disorders 21, 1728–1731.

Huppertz, H.-J., Kroll-Seger, J., Danek, A., Weber, B., Dorn, T., Kassubek, J., 2008. Automatic striatal volumetry allows for identification of patients with chorea-acanthocytosis at single subject level. Journal of Neural Transmission 115, 1393–1400.

Kutcher, J., Kahn, M., Andersson, H., Foundas, A., 1999. Neuroacanthocytosis masquerading as Huntington's disease: CT/MRI findings. Journal of Neuroimaging 9, 187–189.

Leh, S., Pitio, A., Chakravaty, M., Strafella, A., 2007. Fronto-striatal connections in the human brain: a probabilistic diffusion tractography study. Neuroscience Letters 419, 113–118.

Levitt, J.J., Styner, M., Niethammer, M., Bouix, S., Koo, M.S., Voglmaier, M.M., Dickey, C.C., Niznikiewicz, M.A., Kikinis, R., McCarley, R.W., Shenton, M.E., 2009. Shape abnormalities of caudate nucleus in schizotypal personality disorder. Schizophrenia Research 110 (1–3), 127–139.

Looi, J., Lindberg, O., Liberg, B., Tatham, V., Kumar, R., Maller, J., Millard, E., Sachdev, P., Hogberg, G., Pagani, M., Botes, L., Engman, E., Zhang, Y., Svensson, L., Wahlund, L.-O., 2008. Volumetrics of the caudate nucleus: reliability and validity of a new manual tracing protocol. Psychiatry Research: Neuroimaging 163, 279–288.

Looi, J., Svensson, L., Lindberg, O., Zandbelt, B., Ostberg, P., Orndahl, E., Wahlund, L.-O., 2009. Putaminal volume in frontotemporal lobar degeneration and Alzheimer's Disease — differential volumes in subtypes of FTLD, AD, and controls. American Journal of Neuroradiology 30, 1552–1560.

Paniagua, B., Styner, M., Macenko, M., Pantazis, D., and Niethammer, M., 2009. Local shape analysis using MANCOVA. Insight Journal (July–Dec).

Rampoldi, L., Danek, A., Monaco, A.P., 2002. Clinical features and molecular bases of neuroacanthocytosis. Journal of Molecular Medicine 80 (8), 475–491.

Rampoldi, L., Dobson-Stone, C., Rubio, J., Danek, A., Chalmers, R., Wood, N., Verellen, C., Ferrer, X., Malandrini, A., Fabrizi, G., Brown, R., Vance, J., Pericak-Vance, M., Rudolf, G., Carre, S., Alonso, E., Manfredi, M., Nemeth, A., Monaco, A., 2001. A conserved sorting-associated protein is mutant in chorea-acanthocytosis. Nature Genetics 28, 119–120.

Robertson, B., Evans, A., Walterfang, M., Ng, A., Velakoulis, D., 2008a. Epilepsy, progressive movement disorder and cognitive decline. Journal of Clinical Neuroscience 15, 812.

Robertson, B., Evans, A., Walterfang, M., Ng, A., Velakoulis, D., 2008b. Epilepsy, progressive movement disorder and cognitive decline. Journal of Clinical Neuroscience 15, 812.

Rodrigues, G., Walker, R., Bader, B., Danek, A., Marques Jr., W., Tumar, V., 2008a. Chorea-acanthocytosis: report of two brazilian cases. Movement Disorders 23, 2090–2093.

Rodrigues, G., Walker, R., Bader, B., Danek, A., Marques Jr., W., Tumar, V., 2008b. Chorea-acanthocytosis: report of two Brazilian cases. Movement Disorders 23, 2090–2093.

Styner, M., Lieberman, J., Pantazis, D., Gerig, G., 2004. Boundary and medial shape analysis of the hippocampus in schizophrenia. Medical Image Analysis 8, 197–203.

Styner, M., Oguz, I., Xu, S., Brechbuhler, C., Pantazis, D., Levitt, J., Shenton, M., Gerig, G., 2006. Framework for the statistical shape analysis of brain structures using SPHARM-PDM. Insight Journal 1–21.

Tekin, S., Cummings, J., 2002. Frontal-subcortical neuronal circuits and clinical neuropsychiatry: an update. Journal of Psychosomatic Research 53, 647–654.

Ueno, S., Maruki, Y., Nakamura, M., Tomemori, Y., Kamae, K., Tanabe, H., Yamashita, Y., Matsuda, S., Kaneko, S., Sano, A., 2001a. The gene encoding a newly discovered protein, chorein, is mutated in chorea-acanthocytosis. Nature Genetics 28, 121–122.

Ueno, S., Maruki, Y., Nakamura, M., Tomemori, Y., Kamae, K., Tanabe, H., Yamashita, Y., Matsuda, S., Kaneko, S., Sano, A., 2001b. The gene encoding a newly discovered protein, chorein, is mutated in chorea-acanthocytosis. Nature Genetics 28, 121–122.

Utter, A., Basso, M., 2008. The basal ganglia: an overview of circuits and function. Neuroscience and Biobehavioral Reviews 32, 333–342.

Valko, P.O., Hanggi, J., Meyer, M., Jung, H.H., 2010. Evolution of striatal degeneration in McLeod syndrome. European Journal of Neurology 17 (4), 612–618.

Walterfang, M., Yucel, M., Walker, R., Evans, A., Bader, B., Ng, A., Danek, A., Mocellin, R., Velakoulis, D., 2008. Adolescent obsessive–compulsive disorder heralding chorea-acanthocytosis. Movement Disorders 23, 422–425.

Whitwell, J., 2009. Voxel-based morphometry: an automated technique for assessing structural changes in the brain. The Journal of Neuroscience 29, 9661–9664.

Zhao, Z., Taylor, W.D., Styner, M., Steffens, D.C., Krishnan, K.R., MacFall, J.R., 2008. Hippocampus shape analysis and late-life depression. PLoS ONE 3 (3), e1837.

Please cite this article as: Walterfang, M., et al., Shape alterations in the striatum in chorea-acanthocytosis, Psychiatry Research: Neuroimaging (2011), doi:10.1016/j.pscychresns.2010.10.006